

STUDY OF THE PERFORMANCES OF A TANDEM PHOTOVOLTAIC CELL BASED ON CIGS

B. MERAH^{a,*}, H. KHACHAB^b, A. HEMMANI^b, M. BOUSSERHANE^b

^a*ENERGARID laboratory, University of TAHRI Mohammed Bechar, BP 417 Bechar. Algeria*

^b*Departement of matter sciences, Faculty of exact sciences, University of TAHRI Mohammed Bechar, BP 417 Bechar. Algeria*

Solar cells are currently the subject of various research works whose goal is to improve the performance of these cells by minimizing physical losses and achieving the best relationship between energy efficiency and cost. Among the most common types of cells currently, one can find those in thin layers made in CIGS (Copper, Indium, Gallium and Selenium). The objective of this work is within the framework of the numerical modeling of the tandem structure of two thin-film solar cells based on CIGS in order to optimize the physical and geometrical characteristics of the different layers of the cell such as the thicknesses of the layers, gap energy, etc. The studied cell is composed of two parts; an top cell based on CuGaSe₂ and a bottom cell based on CuInSe₂.

(Received November 25, 2018; Accepted January 17, 2019)

Keywords: Photovoltaic Cell, Cigs, Tandem, Performances

1. Introduction

The efficiency of a homojunction solar cell is limited by the multiple losses that occur in this type of cells and in particular those relating to photons and charge carriers (electrons and holes).

It is therefore necessary to use several cells, each being sensitive only in a spectral band, and the whole covering a wider part of the solar spectrum. This is the concept of multispectral conversion.

In this context, we are interested in simulating the performance of multi-function photovoltaic cells based on CIGS material under standard operating conditions.

Our main goal is to analyze the effect of some physical and technological parameters based on their photovoltaic conversion efficiency.

2. Presentation of the tandem cell

The choice of materials for the realization of a tandem structure is guided by the optical and electrical properties of the two materials, in particular by the values of their band gap. The gap of the second cell (CuInSe₂) must allow it the absorption of the radiation transmitted by the first cell (CuGaSe₂) [1-4]. Photons energy is essentially inferior to the gap of the first cell. We present here the possibility of using the CuGaSe₂ / CuInSe₂ structure as a photovoltaic structure [5, 6]. The structure is a tandem of two cells, the first CuGaSe₂ cell is the upper cell and the second CuInSe₂ cell is the lower cell [7]. Between these two cells, there is a tunnel junction as shown in Fig. 1 [7-9].

* Corresponding author: merah.benyoucef@gmail.com

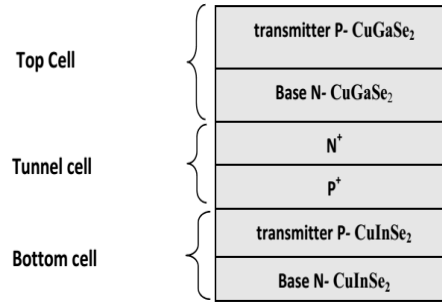


Fig. 1. Structure of the $CuGaSe_2/CuInSe_2$ tandem cell.

3. Photocurrent calculation

3.1. Basic equations

We have put in place the equations that govern the static and dynamic characteristics of the carriers in the semiconductor by assuming that there is no intervention of the magnetic field. Under these conditions, we obtain the following equations [1-5]:

For electrons:

$$\vec{J}_n = qu_n n \vec{E} + qD_n \overrightarrow{\text{grad}} n \quad (1)$$

For holes:

$$\vec{J}_p = qu_p n \vec{E} - qD_p \overrightarrow{\text{grad}} p \quad (2)$$

The continuity equations for the two types of carriers are expressed as follows:

For electrons[7,8]:

$$\frac{dn}{dt} = D_n \frac{d^2 n}{dx^2} - \frac{n}{\tau_n} + G_1(x) \quad (3)$$

For holes:

$$\frac{dp}{dt} = D_p \frac{d^2 p}{dx^2} - \frac{p}{\tau_p} + G_2(x) \quad (4)$$

By neglecting the effect of the electrostatic field outside the depletion zone and assuming that the junctions are stationary (permanent illumination), the continuity equations become:

$$D_n \frac{d^2 n}{dx^2} - \frac{n}{\tau_n} + G_1(x) = 0 \quad (5)$$

$$D_p \frac{d^2 p}{dx^2} - \frac{p}{\tau_p} + G_2(x) = 0 \quad (6)$$

The main objective of our work is to study CIGS tandem photovoltaic cells in order to take the best electrical characteristics of this type of cells such as the photocurrent spectral response, characteristic $I(V)$, the form factor, and photovoltaic conversion efficiency.

3.2. Parameters of the studied cell

The cells are superimposed in decreasing order of the values of the induced band heights E_g , where the device having the highest value is at the top and receiving all the radiation. For a given solar spectrum, and a finite number of materials, there are imposed values of E_g giving maximum efficiency to the system. For this, the chosen parameters are reported in Table 1.

Table 1. Parameters of the studied cell [8-13].

	Upper Cell (top)	Lower Cell (bottom)
Gap Energy E_g (eV)	1.67	1.02
Thickness d (μm)	1.5	2.5
Concentration of Acceptor Atoms N_a (cm^{-3})	5.10^{15}	5.10^{15}
Intrinsic Concentration n_i (cm^{-3})	$1.1.10^{10}$	$1.1.10^{10}$
The effective density of the state of the electrons in the valence band N_c (cm^{-3})	5.10^{18}	5.10^{18}
The effective density of the state of the holes in the valence band N_v (cm^{-3})	10^{19}	10^{19}
The Lifetime of Electrons τ_n (s)	10^{-10}	10^{-10}
Diffusion coefficient D_n (cm^2/s)	3.9	3.9
Length of diffusion L_n (cm)	$6.6.10^{-6}$	$6.6.10^{-6}$
Relative Permittivity ϵ_r	15	15

For the external parameters used, we take standard conditions, which are:

- The AM1.5 solar spectrum.
- The illumination is $1000\text{W} / \text{m}^2$.
- The temperature is 300 K.

4. Results

4.1. Spectral response

The spectral response makes it possible to evaluate the quantum yield of a solar cell as a function of the wavelength of the incident light. This measurement consists in illuminating the solar cell with a monochromatic spectrum that varies in the absorption range of the material [8].

To study the internal mechanisms of the cell, it is necessary to study the variation of the spectral response. For this purpose, it is necessary to consider only the absorbed photons in order to analyze the other parameters of the cell. To do this, we will first proceed in a preliminary study of the spectral response.

In Fig. 2, the variation of the spectral response of the tandem PV cell (both cells) is presented as a function of wavelength for recombination rate values of $10^5 \text{ cm}^2 / \text{s}$ and $10^7 \text{ cm}^2 / \text{s}$.

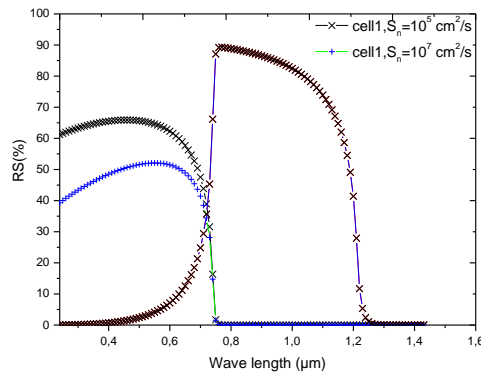


Fig. 2. Variation of the spectral response of the two cells as a function of the wavelength for:
 $E_{g1} = 1.67 \text{ eV}$, $E_{g2} = 1.02 \text{ eV}$, $S_{n1} = 10^6 \text{ cm}^2 / \text{s}$ and $S_{n2} = 10^4 \text{ cm}^2 / \text{s}$.

From Fig. 2, it is clear that much of the absorption spectrum is due to the first cell. On the other hand, the second cell (lower cell) absorbs a portion that is lower than the one absorbed by the upper cell.

It is also noted that the increase in the superficial recombination rate causes a decrease in the spectral response throughout the region of the spectrum absorbed. On the other hand, a slight variation is observed in the second cell (bottom cell).

Therefore, the top cell (cell 1) is the most important in terms of light spectrum absorption. It plays the role of a window layer.

4.2. The effect of gap energy

A. Influence of gap energy on the spectral response

To study the effect of the gap energy on the spectral response, we have plotted in Fig. 3 the variation of the spectral response as a function of the wavelength for different values of the gap energy of the first cell, and fixed the gap of the second cell (lower cell) whose $E_{g2} = 1.02$ eV.

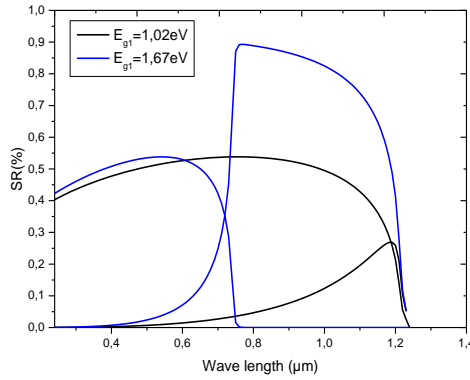


Fig. 3. Variation of the spectral response of the two cells as a function of the wavelength for: $E_{g1} = 1.67$ eV, $E_{g2} = 1.02$ eV, $S_{n1} = 10^6$ cm^2/s and $S_{n2} = 10^4$ cm^2/s .

Table 2 shows the parameters of the two cells (upper and lower) obtained after simulation, by varying the gap energy of the first cell and setting the second gap at 1.02 eV.

Table 2. Characteristics of the two cells.

	Top Cell	Bottom Cell
$S_n(\text{cm.s}^{-1})$	10^6	10^4
$E_g(\text{eV})$	1.67	1.02
$J_{ph}(\text{mA/cm}^2)$	12.8	21.3
$S_n(\text{cm.s}^{-1})$	10^6	10^4
$E_g(\text{eV})$	1.53	1.02
$J_{ph}(\text{mA/cm}^2)$	14.7	18.1
$S_n(\text{cm.s}^{-1})$	10^6	10^4
$E_g(\text{eV})$	1.16	1.02
$J_{ph}(\text{mA/cm}^2)$	21	7.5
$S_n(\text{cm.s}^{-1})$	10^6	10^4
$E_g(\text{eV})$	1.02	1.02
$J_{ph}(\text{mA/cm}^2)$	24.5	3.3

The analysis of the previous results shows that:

- Most of the absorption spectrum is due to the first cell.
- The gap value of cell 1 is greater than that of cell 2.
- The gaps must be chosen in such a way as to absorb the maximum amount of radiation.

B. Influence of gap energy on the photocurrent

Fig. 4 illustrates the photocurrent variation as a function of the gap energy of the upper cell.

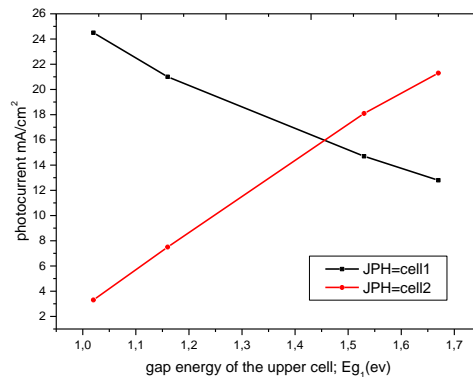


Fig. 4. Photocurrent variation as a function of the gap energy of the upper cell.

In Fig. 4, it can clearly be seen that the increase in gap energy of the first cell (top cell) results in both a decrease in the photocurrent of the first cell and a remarkable increase in the performance of the second cell. The results also show the existence of a point of intersection that represents two optimal values; the first for the photocurrent ($J_{ph1} = J_{ph2} \approx 16 \text{ mA / cm}^2$) and the second for the gap energy $E_{g1} = 1.46 \text{ eV}$.

The increase of the photocurrent causes an increase of the open circuit voltage (lower cell), and the decrease of the photocurrent causes a decrease of the open circuit voltage (case of the top cell), see Fig. 5.

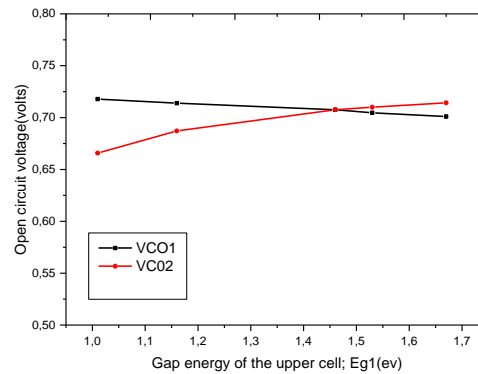


Fig. 5. Variation of the open circuit voltage as a function of the gap energy of the upper cell.

Thus, it is noted that the open circuit voltage is proportional to the variation of the photocurrent in the two cells (top and bottom).

4.3. The Effect of the Transmitter Thickness of the top Cell

After determining the optimal parameters of the two cells, we will see the influence of the thickness of the emitter of the top cell on the photocurrent. The photovoltaic quantities of the two cells are reported in Table 3.

Table 3. Parameters of the cell under study (the thickness of the base and the gap energy).

	Top Cell	Bottom Cell
BaseThickness (μm)	1	1.5
Gap Energy(eV)	1.46	1.02

The influence of the thickness of the emitter of the upper cell on the photocurrent is illustrated in Fig. 6.

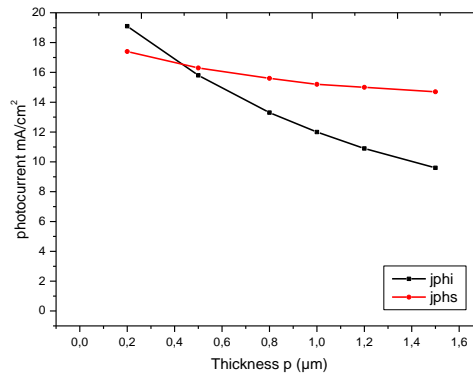


Fig. 6. Influence of the top cell emitter thickness on the photocurrent.

From Fig. 6, it is noted that if the thickness of the emitter of the top cell increases, the photocurrent of the two cells decreases with a very remarkable decrease; this decrease is mainly due to the flow absorbed in the tandem cell

The decrease in the number of photons absorbed in the emitter causes a limitation of the excited charge carriers. The Table 4 illustrates the photocurrent values of the two cells (top and bottom) obtained from Fig. 6 at each thickness value.

Table 4. Photocurrent values of the two cells.

	Top Cell	Bottom Cell
d (μm)	1.5	
J_{ph} (mA/cm ²)	9.6	14.7
d (μm)	1.2	
J_{ph} (mA/cm ²)	10.9	15
d (μm)	1	
J_{ph} (mA/cm ²)	12	15.2
d (μm)	0.8	
J_{ph} (mA/cm ²)	13.3	15.6
d (μm)	0.5	
J_{ph} (mA/cm ²)	15.8	16.3
d (μm)	0.2	
J_{ph} (mA/cm ²)	19.1	17.4

With (d) which represents the thickness of the emitter of the upper cell.

The choice of the thickness of the emitter is a very important step, which must be studied before the value of this thickness strongly influences the performance of the photovoltaic cell. Moreover, it can make the cell more or less efficient.

In order to optimize and identify this thickness, we chose the values of the first points in the two curves $d = 0.43 \mu\text{m}$;

For the second cell (bottom cell), the emitter of the upper cell plays the role of a window layer. The decrease in the thickness of the emitter of the upper cell shows an increase of the photocurrent in the bottom cell. It should be noted that the optimal thickness of the optimum upper cell emitter is equal to $0.43\mu\text{m}$.

4.3. Characteristic J (V)

A. Characteristic J (V) real and ideal

In this part, we will present results on the effects of some parameters on the characteristic J (V), fixing other parameters under the following conditions: $E_{g1} = 1.46\text{eV}$ and $d = 1\mu\text{m}$.

Figs. 7 and 8 respectively represent the characteristics J (V) of the two cells in the ideal and real case.

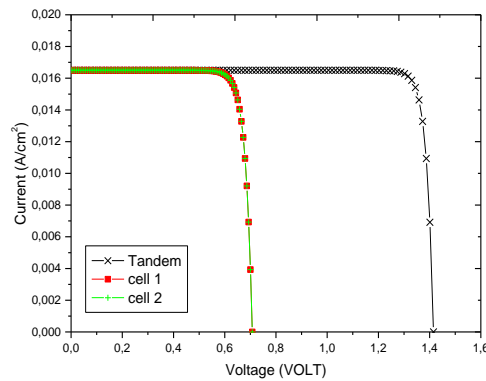


Fig. 7. Characteristic J (V) for the two cells in the ideal case.

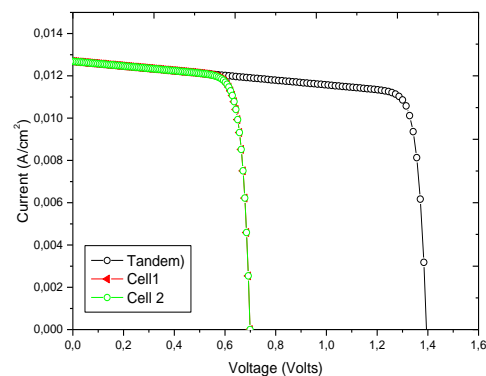


Fig. 8. J (V) characteristic for both cells in the real case.

Both Figs. 7 and 8 show that:

- The two currents (top and bottom cells) are equal in both cases (real and ideal).
- The current supplied by the tandem cell is the lowest current.
- Open circuit voltage (V_{co}) is the sum of the open circuit voltages of each cell.
- For the real case, we notice some degradation (curvature); this is justified by the values of the series and shunt resistors.

In Table 5, the parameters of the cell obtained from Fig. 8 are presented.

Table 5. Ideal values of the parameters of the two cells.

	Top Cell	Bottom Cell
$J_{ph}(\text{mA}/\text{cm}^2)$	16.5	16.5
$V_{co}(\text{V})$	0.707	0.707
$\eta(\%)$	21.2	
FF(%)	90	

B. The effect of the optimized parameters on the characteristic J (V)

Figs. 9 and 10 show the characteristic J (V) for the two cells in the real and ideal cases respectively, with the parameters determined in the preceding parts ($E_{g1} = 1.46\text{eV}$, $d = 0.43\ \mu\text{m}$).

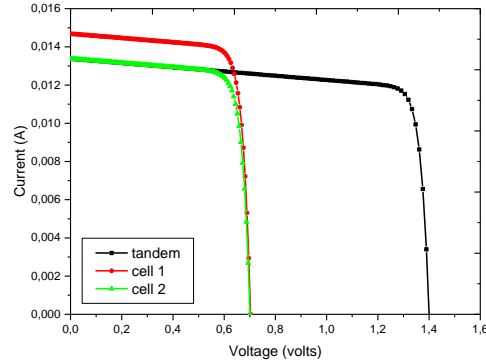


Fig. 9. Characteristic J (V) for the two cells in the real case.

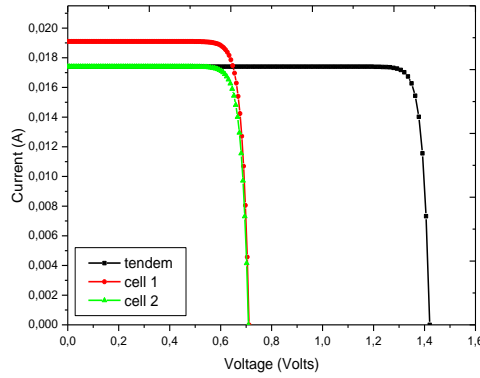


Fig.10. Characteristic J (V) for both cells in the ideal case.

The analysis of Figs. 9 and 10 shows that, the open circuit voltage (V_{co}) is the sum of the open circuit voltages of each cell.

In tables 6 and 7, we illustrate the photovoltaic quantities obtained from the simulation of the two cells (in both real and ideal case).

Table 6. Photovoltaic quantities of the real cell ($R_s = 0.3\ \Omega$ and $R_{sh} = 900\ \Omega$).

	Top Cell	Bottom Cell
$J_{cc}(\text{mA}/\text{cm}^2)$	14.7	13.4
$V_{co}(\text{V})$	0.703	0.700
$\eta(\%)$	15.12	
FF(%)	80.5	

Table 7. Photovoltaic quantities of the ideal cell.

	UpperCell	LowerCell
$J_{cc}(\text{mA}/\text{cm}^2)$	19.1	17.4
$V_{co}(\text{V})$	0.711	0.708
$\eta(\%)$	22.48	
FF(%)	90.5	

4.4. Photovoltaic conversion efficiency

In this last part of the results section, we are interested in the study of the variation of the photovoltaic conversion efficiency as a function of the gap energy under the optimization conditions mentioned in the previous paragraphs Fig. 11.

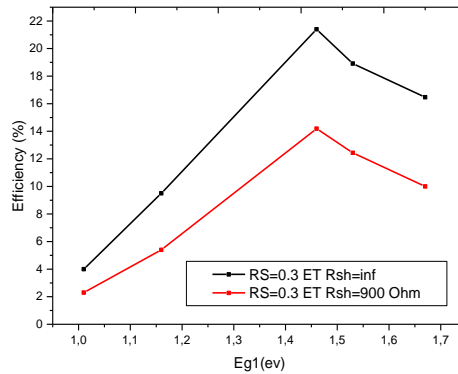


Fig. 11. Variation in photovoltaic conversion efficiency versus gap.

Fig. 11 shows the existence of an optimal gap (1.46 eV) whose conversion efficiency is better.

5. Conclusions

The results presented in this work were made to optimize the best performances and parameters of the tandem cell based on CIGS. The analysis of the results obtained from our simulations shows that:

- The current supplied by the tandem cell is the weakest current;
- The open-circuit voltage is the sum of the open-circuit voltages of the two cells;
- The thickness of the transmitter is 0.43 μm ;
- There is an optimal gap of 1.46 eV.

References

- [1] S. R. Wenham, M. A. Green, M. E. Watt, Applied Photovoltaic, Bridge Printer, Sidney, 1994.
- [2] S. M. Sze, Physics of semiconductor Devices, second edition, John, Wiley and Son, Inc., 1981.
- [3] U. P. Singh, S. P. Patra, Progress in Polycrystalline Thin-Film Cu(In,Ga)Se₂ Solar Cells, 2010.
- [4] M. A. Green, K. Emery, Y. Hishikawa, W. Warta, Prog. Photovolt. Res. Appl. 18, 144 (2010).
- [5] P. Chelvanathan, M. I. Hossain, N. Amin, Current Appl. Phys. 10, S387 (2010).
- [6] U. P. Singh, S. P. Patra, Progress in Polycrystalline Thin-Film Cu(In,Ga)Se₂ Solar Cells, 2010.
- [7] Dennai Benmoussa, Modélisation d'une cellule solaire en mode dichroïque, magister thesis, University of Bechar, Algeria, French, 2011.

- [8] M. Bousserhane, Etude des performances d'une cellule solaire tandem à base de CIGS, Master thesis, University of Bechar, French, 2014.
- [9] B. Hassane, D. Benmoussa, Journal of Nano- and Electronic Physics 10(5), 05044 (2018).
- [10] M. K. Selma, Etude et simulation de cellules photovoltaïque a couches minces à base de CIS et CIGS, magister thesis, University of Abou-BakrBlekaid, Tlemcen, Algeria, 2012.
- [11] A. Duchatelet, Synthèse de couches minces de Cu(In,Ga)Se₂ pour cellules solaires par électro-dépôt d'oxydes mixtes de cuivre-indium-gallium, Doctorat thesis, University of Lille, French, 2012.
- [12] L. Ribeaucourt, Electro-dépôt et sélénisation d'alliages Cu-In-Ga en vue de la synthèse de couches minces de Cu(In,Ga)Se₂ pour cellules solaires, Doctorat thesis, University of Pierre et Marie curie, French, 2011.
- [13] S. Fatma-Zohra, Modélisation d'une cellule solaire en couche mince à base de Cuivre Indium Sélénium(CuInSe₂), Magister thesis, University of Kasdi Merbah, Ouargla, Algeria, French 2009.